

Performance Evaluation of Fenton Based Processes in Reducing COD of the Petroleum Effluents Using the Waste of Steel Slag

Fatemeh Etemadiasl

Shahid Chamran University of Ahvaz

Parvaneh Tishehzan (✉ ptishehzan@yahoo.com)

Shahid Chamran University of Ahvaz <https://orcid.org/0000-0002-5283-1047>

Seyed Mahmood Kashefipour

Shahid Chamran University of Ahvaz

Nematolah Jaafarzadeh Haaghighifard

Ahvaz Jondishapour University of Medical Sciences

Research Article

Keywords: EF, PF, PEF, COD, Taguchi, Steel slag, Petroleum effluent

Posted Date: January 18th, 2022

DOI: <https://doi.org/10.21203/rs.3.rs-1033579/v1>

License:  This work is licensed under a Creative Commons Attribution 4.0 International License.

[Read Full License](#)

26 Advanced oxidation was first used for water treatment in 1980 (Glaze, 1987; Glaze, Kang and Chapin, 1987). AOP
27 processes are based on processes that produce an appropriate amount of active radicals such as hydroxyl radical
28 (OH°), radical ($\text{SO}_4^{\circ-}$) and oxygen radical (O°) (Cho *et al.*, 2005; Ikai *et al.*, 2010; Deng and Zhao, 2015).

29 Since hydroxyl radicals have high oxidizing power ($E^\circ = 2.8 \text{ V}$), they remove most contaminants (especially
30 organic contaminants). These methods are more capable of treating toxic contaminants, usually do not have the
31 problem of surplus disposition and waste, are performed at room temperature and atmospheric pressure and are
32 relatively inexpensive, and also the reaction speed is fast (Gaya and Abdullah, 2008). Advanced oxidation such as
33 photochemical oxidation, wet catalytic oxidation, sonochemical oxidation, O_3 oxidation, electrochemical oxidation
34 and Fenton oxidation are widely used for direct mineralization of organic contaminants or to improve the
35 degradability of organic contaminants (Bokare and Choi, 2014; Sharma, Ahmad and Flora, 2018). Compared to
36 other advanced oxidation processes, Fenton processes are the most popular due to some significant advantages such
37 as wide application range, strong anti-interference ability, simple operation, fast degradation and mineralization
38 (Chen *et al.*, 2011; Wang *et al.*, 2016).

39 Various factors such as temperature, pH, H_2O_2 concentration, iron ion content, contact time, etc. affect the efficiency
40 of Fenton-based processes (Stepnowski *et al.*, 2002; Meriç, Kaptan and Ölmez, 2004; Mousavi *et al.*, 2010;
41 Jaafarzadeh, Ghanbari and Moradi, 2015; Lopez-Saavedra *et al.*, 2018). Performance of Fenton-based processes are
42 differen; Comparison between Fenton, EF, Sono-Electro-Fenton (SEF) and PEF processes for phenol removal
43 showed that the degradation efficiency of the processes is as follows: $\text{PEF} < \text{SEF} < \text{EF} < \text{Fenton}$ (Babuponnusami
44 and Muthukumar, 2012a). In the Photo Catalysis / PEF hybrid system 85% of TOC and 96% of COD were removed
45 from effluent containing Polyaniline (Ou *et al.*, 2019).

46 Testing all the parameters for different Fenton process requires a lot of time and cost, but in such cases, the
47 experiment design method can be used. The Taguchi method is one of the experiment design that compared to factor
48 methods provides advantages such as less number of experiments and therefore less cost and time of testing, the
49 ability to evaluate the interaction effects and conducting experiments in parallel and ultimately predicting the
50 optimal response. In general, this method reduces the number of experiments required for optimization and increases
51 the accuracy of the results. The most important and effective factor can be determined with this method (Yonar and
52 Kurt, 2017; Suraj *et al.*, 2019) One of the important issues in electrochemical processes is selecting the right
53 electrode (especially anode). The anodes such as BDD⁵, Pt, and DSA⁶ due to produce more powerful (OH°) have
54 shown their high potential in removing various contaminants (Villanueva-Rodríguez *et al.*, 2014; Brillas and
55 Martínez-Huitle, 2015; Flores *et al.*, 2016; Steter, Brillas and Sirés, 2016; Komtchou *et al.*, 2017; Moreira *et al.*,
56 2017; Aveiro *et al.*, 2018; Guelfi *et al.*, 2019; Thiam and Salazar, 2019; Ye *et al.*, 2019). Some studies have
57 investigated the effect of the similar cathode and anode electrode (such as identical electrodes of Na_2SO_4
58 (Babuponnusami and Muthukumar, 2012b); graphite electrodes (Nidheesh and Gandhimathi, 2014) and identical
59 BDD electrodes (Villanueva-Rodríguez *et al.*, 2014) in the Fenton based processes and achieved good results.

⁵ Boron-doped diamond

⁶ Dimensionally stable anodes

60 Khuzestan province in southwestern Iran has large industries such as petroleum and steel industries. High pollution
61 of the effluents of petroleum industry desalination units and the presence of high slag in the steel industry are among
62 the environmental problems of this region.

63 Since, in novel research, the use of solid iron catalysts or iron-modified cathodes with it has shown good
64 performance (Brillas, 2020), therefore steel slag (containing iron compounds) was used as catalysts and electrodes.
65 The present study aimed to compare different Fenton-based processes in reducing pollution of petroleum industry
66 effluents by using waste materials (steel industry slag). Also, the most effective parameters for reducing COD were
67 identified in each of the processes using the Taguchi method.

68 **2. Materials and methods**

69 This study was designed and implemented to evaluate the efficiency of Fenton, PF, EF and PEF processes in
70 reducing COD from effluents of petroleum desalination unit and, the effect of factors such as pH, contact time,
71 catalyst content, hydrogen peroxide content, radiant intensity and current on the reduction efficiency of COD was
72 investigated. The measured parameters of the effluent of one of the desalination units, by the petroleum-rich areas of
73 the south have been presented Table (1). The catalysts for all four processes of F, EF, PF and PEF were selected
74 from fine particle slag; also cupal slag because of its nature was used as the cathode and anode for EF and PEF
75 processes. According the XRF analysis (Table 2), the compounds of iron oxide and calcium oxide have the highest
76 amount. The experiments were designed using Taguchi orthogonal array and Minitab 18 software. The results of the
77 experiments were analyzed using Microsoft Office Excel and Minitab 18 software using two types of signal analysis
78 to noise and variance.

79 *2.1. Experiment design*

80 The Taguchi method minimizes the number of experiments required using orthogonal arrays. Array L_9 (3^4) was
81 used to determine the appropriate conditions based on this statistical model; this means that 4 effective parameters
82 were selected as arrays and examined at three levels, as shown in Tables (3).

83 Achieving optimal conditions for a specific objective in Taguchi method is based on the signal to noise index S/N.
84 S/N is the transformed value of the loss function used to measure the deviation of the performance characteristic
85 from the ideal value. The higher S/N indicate the better performance of the system (Gönder *et al.*, 2010). The
86 calculation method of S/N is selected according to the intended optimization type. Here, according to the goal of
87 achieving the maximum range, S/N of "larger is better" type was used (Milkey *et al.*, 2014).

88 *2.2. Required solutions*

89 Solutions of sulfuric acid (98.08%), nitric acid (63.01%), sodium hydroxide (98%) for pH adjustment according to
90 Taguchi orthogonal arrays design and H_2O_2 concentration (29-31%) were prepared from Merck Germany for
91 experiments.

92 *2.3. Reactor used*

93 All experiments related to Fenton were performed on a 1250-cc beaker with a diameter of 90 mm and a height of
 94 150 mm. To perform the PF test, a black box designed from wood was used to prevent the radiation from
 95 penetrating into the medium and to have a higher efficiency. In order to produce radiation from 4 UV-C lamps with
 96 a wavelength of 200 to 280 nm each with a power of 8 watts and a total of 32 watts, were installed vertically on all
 97 four sides of the box and a glass beaker with a volume of 1250 ml was placed exactly in the middle of the box so
 98 that of radiation should be uniformly reflected on the sample from each side. To perform an EF test, a Pyrex beaker
 99 with a volume of 1250 ml was used as the reaction medium, and the cathode and anode, both made of Cupal slag,
 100 were placed in unknown shapes at a distance of 3 cm from each other. The power supply in this experiment was a
 101 variable voltage device of DAZHENG model PS-302 D with variable current characteristics of 0 to 2 amps and
 102 variable voltage of 0 to 30 volts. The required catalyst content and the required hydrogen peroxide (according to the
 103 required level) were added to each sample. In the combined state of PEF, two small holes (with the size of a wire)
 104 are made in the upper part of the black box, and the power cords of the cathode and anode are passed through them
 105 and connected to the AC power supply.

106

107

108

109

110

111

112

113

114

115

116

117

118

Table 1. Chemical properties of petroleum effluent used

parameters	Amounts	the unit	parameters	Amounts	the unit	parameters	Amounts	the unit
-------------------	----------------	-----------------	-------------------	----------------	-----------------	-------------------	----------------	-----------------

SO_4	410	ppm	PO_4	1.3	ppm	pH	5.33	-
F	4.5	ppm	NO_3	1.55	ppm	TDS	181000	ppm
CO_3	less than 0.1	ppm	NO_2	0.15	ppm	EC	362000	$\mu S/cm$
HCO_3	9	ppm	Cl	102930	ppm	COD	More than 10000	ppm
Bi	less than 0.1	ppm	Ba	less than 0.1	ppm	Ag	less than 0.1	ppm
Ca	60804	ppm	Be	Less than 0.2	ppm	Al	less than 100	ppm
Co	less than 1	ppm	Ce	less than 1	ppm	Cd	less than 0.1	ppm
Mg	6243	ppm	Fe	342	ppm	Cr	4	ppm
Li	41	ppm	Mo	less than 0.3	ppm	Cs	Less than 0.5	ppm
K	4993	ppm	Mn	6	ppm	Cu	less than 3	ppm
P	10	ppm	Zn	5	ppm	Na	less than 10	ppm
Pb	3	ppm	Ni	2	ppm	V	5	ppm
						S	972	ppm

119

120

Table 2. XRF analysis related to Khuzestan steel slag

Sample slag	SiO_2	Al_2O_3	Fe_2O_3	Ca O	Na_2O	M gO	K_2O	T iO_2	M nO	P_2O_5
%	12.48	2.16	32.433	23.368	0.339	4.647	0.083	1.2	0.355	0.307

121

122

123

Table 3. Variables and levels

Fenton	pH	Level 1	Level 2	Level 3
		3	5	7

	H_2O_2(mmol/l)	5	10	15
	Catalyst (gr/l)	5	7.5	10
	Time (min)	30	60	90
Photo-Fenton	pH	3	5	7
	H_2O_2(mmol/l)	5	10	15
	Catalyst (gr/l)	5	7.5	10
	UV(W)	16	24	32
Electro-Fenton	pH	3	5	7
	H_2O_2(mmol/l)	5	10	15
	Catalyst (gr/l)	5	7.5	10
	Voltage (V)	5	15	30
Photo-Electro-Fenton	pH	3	5	7
	H_2O_2(mmol/l)	5	10	15
	Catalyst (gr/l)	5	7.5	10
	UV(W)	16	24	32
	Voltage (V)	5	15	30
	Time (min)	30	60	90

124

125 *2.4. Test Method*

126 For Fenton-based processes, the required amount of slag as catalyst, cathode and anode was washed and then dried
127 in an oven at 105 °C for 2 hours. Hydrogen peroxide and 0.1 N sodium hydroxide solutions were prepared. Then the
128 pH value was adjusted using sulfuric acid and 0.1 N sodium hydroxide (portable pH meter model 330 I - WTW
129 Germany). Certain catalyst content (weighed with a Japanese GF300 scale with an accuracy of 0.001 g) and
130 hydrogen peroxide were added to the samples and the retention times according to the intended levels were applied
131 using a stopwatch. After performing experiments related to Fenton process and complementary experiments, the
132 time parameter of 60 minutes was considered as the optimal parameter for PF and EF processes.

133 To perform the PF test, the cathode and anode were both made of slag in unknown shapes placed at the distance of 3
134 cm. The required catalyst content and required hydrogen peroxide (Table 3) was added to each test sample and, the
135 required retention time was applied.

136 Before and after the experiments, a certain volume of sample was taken and the COD content was measured using a
137 spectrophotometer (Hach 5000) by closed reverse digestion (600 nm wavelength). Then the percentage of COD
138 removal was calculated according to Equation (1).

139 (1) Removal percentage = $100 \times \frac{C_0 - C_1}{C_1}$

140 Where C_0 and C_1 present the initial and final concentrations of COD, respectively.

141 2.5. Statistical analysis of data

142 After the experiments, signal-to-noise analysis and analysis of variance were performed on the removal percentages
143 obtained using Mintab18 software. The following equation was used for S/N analysis (Oh *et al.*, 2005):

144 (2)
$$\frac{S}{N} = -10 \log \frac{\sum_{i=1}^r \frac{1}{y_i^2}}{r}$$

145 Where y_i represents the response value for each experiment and r denotes the number of repetitions of each
146 experiment.

147 3. Results and discussion

148 The Taguchi method provided 9 experiments for each of the Fenton, PF and EF methods and 27 experiments for the
149 combined PEF method. The experiments were performed and the results were analyzed using MINTAB 18 software.

150 3.1. Fenton

151 Table (4) shows the average COD removal rate at different levels of each factor and Figure (1-a) displays the main
152 effects for the signal-to-noise ratio in Fenton experiments. The highest and lowest removal percentages in the 9
153 experiments were 73.99% and 26.81%, respectively. Considering the range of slope variation, it can be said that the
154 hydrogen-oxygen parameter has been the most effective factor on the Fenton process. The appropriate levels for
155 each of the factors influencing the process are at the highest point, or the so-called highest signal-to-noise ratio,
156 which, will result in the highest COD removal rate when applied. Therefore, the appropriate conditions to achieve
157 the maximum response value are when pH = 7, H_2O_2 = 10mmol/l, catalyst = 10gr/l and time is 60 minutes.
158 Experimental factors in terms of maximum impact can be ranked according to the delta value (difference between
159 the highest and lowest signal-to-noise values). Therefore, after hydrogen peroxide factor, pH, catalyst and time
160 factors had the greatest effect on COD removal percentage, respectively (Figure (1-a) and Table 4).

161 Basically, the optimal contact time is a very important parameter in chemical reactions and if it exceeds the optimal
162 limit, the process will no longer be economic (Coelho *et al.*, 2006). The optical contact time of 60 min obtained in
163 some other research (Byrappa *et al.*, 2008).The highest COD removal percentage occurs at pH 7 for the Fenton

164 process. However, some previous studies have shown that the Fenton process in the acidic state shows better
 165 performance (Wang *et al.*, 2016).The contaminant adsorption rate on the catalyst surface increases with increasing
 166 the number of catalyst particles and the available surface area, which leads to the production of more hydroxyl
 167 radicals (Tony *et al.*, 2009). By increasing the concentration of hydrogen peroxide from 5 to 10 mmol/L, the COD
 168 removal percentage increases and then decreases with increasing H₂O₂ to 15 mmol/L. Excess concentration of H₂O₂
 169 can act as a hydroxyl radical scavenger. It acts instead of a hydroxyl radical, HO₂•, which has less oxidizing ability
 170 and longer life compared to OH• (Xing, Sun and Yu, 2010).

171 **Table 4. The average response value at different levels of each factor**

		Level 1	Level 2	Level 3	Delta	grade
Fenton	pH	51.75	40.72	65.63	24.91	2
	H₂O₂(mmol/l)	37.21	69.5	51.39	32.28	1
	Catalyst (gr/l)	44.9	48.48	64.73	19.83	3
	Time (min)	51.05	54.99	52.07	3.94	4
Photo-Fenton	pH	72.35	62.54	29.45	42.9	1
	H₂O₂(mmol/l)	65.92	52.66	45.76	20.15	3
	Catalyst (gr/l)	46.04	55.48	62.82	16.78	4
	UV(W)	45.95	51.6	66.8	20.85	2
Electro-Fenton	pH	56.51	63.55	66.19	9.68	4
	H₂O₂(mmol/l)	86.13	35.03	65.09	51.11	1
	Catalyst (gr/l)	69.81	60.29	56.15	13.66	3
	Voltag (V)	57.34	71.2	57.71	13.85	2
Photo-Electro-Fenton	pH	73.04	74.38	71.15	3.23	6
	H₂O₂(mmol/l)	65.09	82.17	71.31	17.08	3
	Catalyst (gr/l)	79.63	63.84	75.09	15.79	4
	UV(W)	64.06	79.38	75.12	15.32	5
	Voltag (V)	61.81	80.19	76.57	18.39	2
	Time (min)	54.3	84.68	79.6	30.38	1

172

173 *3.2. Photo-Fenton*

174 The maximum and minimum chemical oxygen demand in 9 experiments were 86.39 and 12.30%, respectively. The
 175 average COD removal rate at each level and for each factor has been shown in Table (4) and the main effects for the
 176 signal-to-noise ratio have been shown in Figure (1-b).

177 According to Figure (1-b), the most effective factor in the PF process was pH. Delta values in Table (4) also show
 178 that after pH, the most important factors are radiant intensity, hydrogen peroxide and catalyst, respectively. The

179 appropriate levels for each of the factors influencing the process are at the highest point or so-called maximum
 180 signal-to-noise ratio. Therefore, the best conditions for PF test are pH = 3, H₂O₂ = 5mmol/l, catalyst = 10gr/l and
 181 radiant intensity is 32 watts.

182 As the radiant intensity increases, the potential for hydroxyl radical generation increases, resulting in higher COD
 183 removal rate. According to the diagram, it can be said that the optimal radiant intensity is equal to 32 watts. This
 184 finding is consistent with a study by Chinese researchers (using a 30-watt lamp) for the PF process. (Tambosi *et al.*,
 185 2006). The most effective factor in this experiment was pH, which obtained the best conditions at an acidic value of
 186 pH = 3 unlike Fenton. The effect of this parameter on the PF process has been expressed differently in previous
 187 research. Some have preferred acidic pH (Dehghani *et al.*, 2014) and some alkaline pH (Xing, Sun and Yu, 2010).
 188 Therefore, after pH, factor radiant intensity, hydrogen peroxide and catalyst factors had the greatest effect on COD
 189 removal percentage, respectively (Figure (1-b) and Table 4). The hydrogen peroxide content at the lowest
 190 experimental value has given the best result which is consistent with other research (Dehghani *et al.*, 2014). The
 191 amount of HO₂• (which has less oxidizing ability) increase at high level of H₂O₂ (Xing, Sun and Yu, 2010). As
 192 with the Fenton process, the highest COD removal rate is associated with the highest catalyst content.

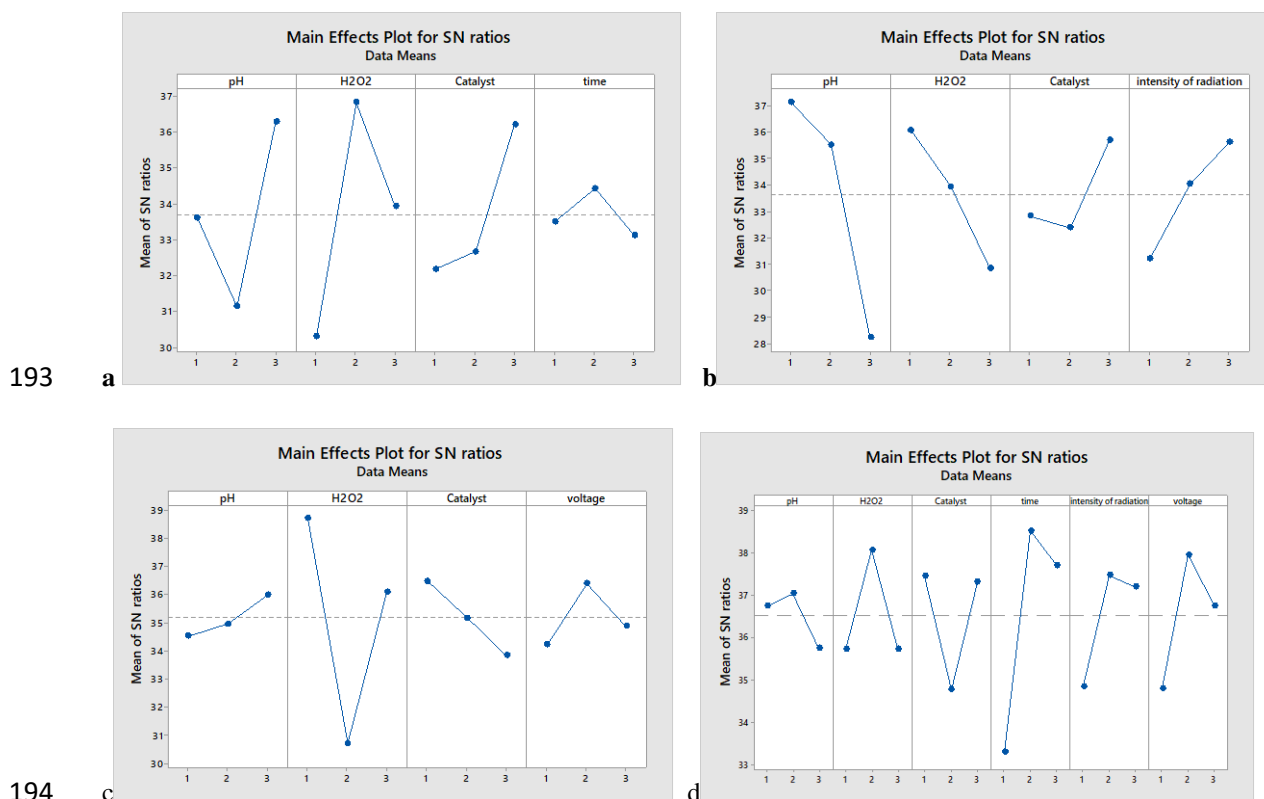


Fig. 1. Diagram of the main effects for the signal-to-noise ratio related to the COD removal percentage.

a) Fenton process, b) PF process c) EF process, d) PEF process

3.3. Electro-Fenton

198 9 experiments were performed for the EF process, the highest and lowest COD removal rates were 93.42% and
199 25.82%, respectively. Table (4) and Figure (1-c) show the average COD removal rate at each level for each factor
200 and the main effects for the S/N ratio. Given the signal-to-noise for each level of factors (Figure 1-c), the appropriate
201 conditions for achieving the maximum response value are when the pH factors are at the third level (pH = 7), the
202 voltage is at the second level (15 volts), and the hydrogen peroxide and the catalyst contents are in the first level (5
203 mmol/l and 5 g/l, respectively).

204 The most effective factor is hydrogen peroxide and after that catalyst, voltage and pH, respectively, were effective
205 on the EF process in the COD removal percentage (Figure 1-c). As with Fenton and PF conditions, the lowest
206 hydrogen peroxide content has had the best response. But in the case of the catalyst in this process, these two
207 reversal processes of Fenton and PF, lower catalyst content has provided more appropriate results. The pH, similar
208 to the Fenton process, has performed better under neutral conditions.

209 *3.4. Photo-Electro-Fenton*

210 According to Taguchi design for this process, 27 experiments were performed. The highest COD removal rate was
211 98.78% and the lowest was 14.59%. Table (4) shows the average COD removal rate at different levels of each factor
212 and Figure (1-d) shows the main effects for the signal-to-noise ratio in PEF experiments.

213 According to the slope of variations in Figure (1-d), it can be said that the most effective factors are time, voltage,
214 catalyst, radiant intensity, hydrogen peroxide and pH, respectively. In this experiment, the highest COD removal
215 rate will occur when the optimal conditions for achieving the maximum response value include pH = 5, H₂O₂ = 10
216 mmol/l, catalyst = 5gr/l, 24 watt radiant intensity, 15 voltage and 60 minutes time.

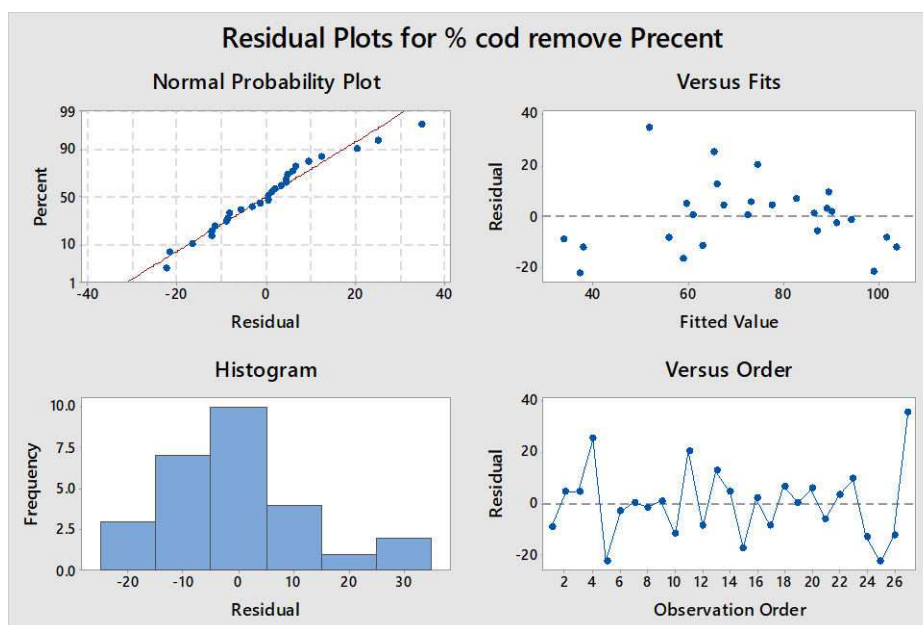
217 Statistical analysis was performed to confirm the results of Taguchi method. Given the number of experiments
218 performed on different processes, this study was feasible for the PEF process. Analysis of linear model of variance
219 was performed for signal-to-noise ratio values and mean COD (Table 5). The results of multivariate analysis of
220 variance showed that the time factor is significant at the level of one percent and the other parameters do not have a
221 significant effect on the output variable. The study of the main effects of S/N ratio also showed a large effect of the
222 time parameter. The R² value of the linear model was 61.65% and the S value was 10.7354. The parameter S is used
223 instead of R² to compare the suitability of models without any constant. The value of S is measured in response
224 variable units and indicates how much the data values fall from the corresponding values. The lower the S value, the
225 better the model describes the response. However, a low value of S or a high value of the coefficient of
226 determination do not in themselves indicate that the model conforms to the assumptions of the model; The residual
227 diagrams should be examined to validate the hypotheses (Figure 2). According to Figure (2), the residual values
228 have been placed around the zero line, indicating the accuracy of the model. As observed in the NPP diagram, the
229 points are almost on a straight line, indicating that the data is approximately normal. The residual versus order
230 diagram is plotted for the independence of the observations. Given that the data are located around the horizontal
231 axis, it can be said that our observations are completely independent and there is no correlation between them.
232 According to the versus Fits diagram, it can be said that the assumption that the variances are constant is accepted.

233 The shape of the histogram has a positive or straight skew. This means that the data have dissymmetry relative to the
 234 mean, and the larger data lead to the lower frequency.

235 **Table 5. Analysis of variance for signal to noise ratio and COD values**

Source	S/N			COD		
	DF	Seq SS	P	DF	Seq SS	P
pH	2	8.332	0.682	2	47.3	0.931
H2O2	2	33.093	0.245	2	1344.7	0.167
Catalyst	2	40.981	0.182	2	1189.1	0.201
time	2	142.693	0.009	2	4765.7	0.007
UV	2	37.218	0.209	2	1125.4	0.217
Voltage	2	45.613	0.153	2	1707.2	0.111
Residual error	14	148.541		14	4616.3	
Total	26	456.471		26	14795.9	

236



237

238 **Fig. 2. Residual diagrams for COD removal percentage**

239 Then, Tukey test was used to find the factor or factors that have a significant difference with other factors.

240 Table (6) shows a Tukey pairwise comparison at the 95% confidence level. The results of Tukey test also showed
241 that the factor of time has a significant difference with other factors for COD removal in the PEF process.

242 3.4.1. Effect of experimental variables (PEF)

243 3.4.1.1 Effect of pH

244 Considering previous researches, little information is available on the performance of the heterogeneous PEF
245 process. On the other hand, in these studies, most experiments have been performed on acidic pH (where catalysts
246 can be partially dissolved) (Khataee, Zarei and Asl, 2010; Khataee and Zarei, 2011; Mousset *et al.*, 2017; Flores *et*
247 *al.*, 2018; Oriol *et al.*, 2019; Ou *et al.*, 2019; Ye *et al.*, 2019). Thus, the efficiency of this process in neutral pH was
248 also investigated. Experiments demonstrated that Fenton and EF processes performed best in neutral conditions and
249 PF and EPF processes in acidic conditions. In PEF process, the rate of COD removal (due to reduced hydroxyl
250 radical production) decreases near neutral. However, a decrease in system performance is observed at very low pH
251 due to dissolution. This matter has been confirmed in previous research (Zhang *et al.*, 2009; Coronado *et al.*, 2013).

252 3.4.1.2 Effect of voltage

253 In the hybrid mode of the PEF process, the voltage level of 15 volts is optimal which is also economical in terms of
254 energy consumption. Therefore, it can be said that in the PEF process, compared to the EF process, the COD
255 removal efficiency has increased due to the use of radiation by applying a suitable voltage.

256

257

258

259

260

261

262

263

264

265

266

267

268 **Table 6. Tukey pairwise comparison at 95% confidence level (COD removal in PEF process)**

Parameter	level	N	Avarage	Group
pH	2	9	74.3771	A
	1	9	73.0413	A
	3	9	71.1509	A
H2O2	2	9	82.17	A
	3	9	71.3064	A
	1	9	65.0929	A
Catalyst	1	9	79.6327	A
	3	9	75.092	A
	2	9	63.8446	A
Time	2	9	84.6752	A
	3	9	79.5962	A
	1	9	54.2979	B
UV	2	9	79.3821	A
	3	9	75.1239	A
	1	9	64.0633	A
Voltage	2	9	80.194	A
	3	9	75.5676	A
	1	9	61.8077	A

* Averages with different letters are significantly different from the others

269

270 3.4.1.3 Effect of catalyst

271 The experiments showed that the optimum amount of catalyst in this process is equal to 5 g/l. The COD removal
272 decreased for the catalyst amount of 7.5 g/l, and it increased again for the amount of 10 g/l. This final result being
273 not consistent with the published data by Byrappa et al. (Byrappa *et al.*, 2008). Because of the amount of
274 contaminants absorbed on the catalyst surface decreased with the increasing number of catalyst particles. It can be
275 said that in general, when the amount of catalyst exceeds the optimum value, due to the turbidity of the environment,
276 UV rays do not effectively reach the surface of the catalyst, and thus the removal efficiency decreases. The
277 conditions of our study are consistent with Bayat et al. (BAYAT, EBRAHIMI and KEYVANI, 2013) in terms of
278 process and acidic environment.

279 3.4.1.3 Effect of H₂O₂

280 According to Figure (1-b), the rate of 10 mmol/l is optimal for hydrogen peroxide which is consistent with the
281 research by Felebuegu and Ezenwa (Ifelebuegu and Ezenwa, 2011). They were able to perform wastewater
282 treatment operations during the Fenton-like oxidation process with this amount of hydrogen peroxide and other
283 optimal conditions. Since the concentration of HO₂• is higher than OH• in solution, the ability of any reactions of

284 HO₂• is prevalent. It should be noted HO₂• has lower oxidizing ability and a longer lifetime than OH• (Tony *et*
285 *al.*, 2009).

286 3.4.1.4 Effect of radiation intensity

287 Obviously, with increasing radiation intensity, the potential for hydroxyl radical production increases, and thus it
288 causes for increasing the removal efficiency of COD. However, by increasing the radiation from 24 watts to 32
289 watts, due to the high concentration of organic matter, contaminants settle on the catalytic surface and prevent light
290 from reaching the catalyst, ultimately reducing the photocatalytic removal (Takeuchi, Hidaka and Anpo, 2012). As a
291 result, according to Figure (1-d), it can be said that the optimal radiation intensity is equal to 24 watts, which is
292 consistent with the research of Xing and Sun (Xing, Sun and Yu, 2010).

293 3.4.2.5 Effect of contact time

294 The COD removal rate increases with increasing contact time. This increased time cause for more photon absorption
295 by the catalyst surface and stimulate the photocatalyst, resulting in more free radical generation of OH• and higher
296 removal efficiency. As shown in Figure (1-d), the S/N value increases significantly with increasing time to level 2
297 (60 minutes) and then decreases.

298 The optimal contact time in the PEF process for COD removal is 60 minutes. The contact time is a very important
299 parameter in chemical reactions, and if it exceeds the optimal limit, it will not be an economic process (Oh *et al.*,
300 2005). However, it should be noted that with increasing time, the pores of the cathode surface fill with contaminate,
301 which reduces the production of H₂O₂ and ultimately reduces the removal efficiency. Babuponnusami and
302 Muthukumar (Babuponnusami and Muthukumar, 2012a), compared different Fenton processes, and found that the
303 amount of pollutant degradation in the PEF process is higher which is consistent with our study.

304 3.5. Comparison of the efficiency of different processes for COD removal

305 In order to evaluate the efficiency of PEF process, the role of Fenton, PF, EF processes on the COD removal was
306 investigated under the conditions of the highest removal percentage obtained. The effect of different processes on
307 COD removal efficiency has been shown in Figure (3). According to Figure (3), it can be seen that PEF, EF, PF and
308 Fenton, respectively, have high efficiency of removing COD from the desalination unit effluent samples. On
309 average, they have between 70 and 100 percent COD removal capability. It seems that dissolved iron in the studied
310 effluent has helped to increase the production of H₂O₂ (especially in electrochemical processes) (Ganiyu, Zhou and
311 Martínez-Huitle, 2018; Nidheesh, Zhou and Oturan, 2018).

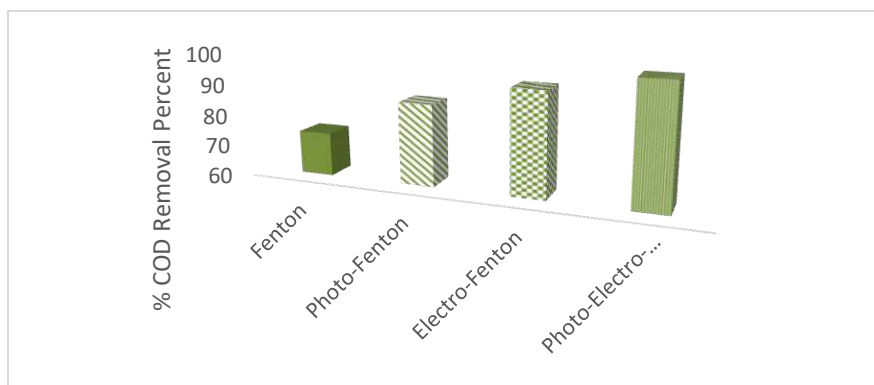


Fig. 3. The COD removal rate in various processes

312

313

314

315 **4. Conclusion**

316 Among the numerous advanced oxidation processes to reduce the chemical oxygen demand of petroleum effluents,
 317 Fenton-based methods are prominent. The chemical oxygen demand (COD) in the petroleum contaminated effluent
 318 during Fenton, PF, EF and PEF processes under the conditions of maximum removal is 74%, 86.39%, 93.42% and
 319 98.781%, respectively, which shows that the combined PEF process with the highest rate of COD removal has a
 320 greater ability to mineralize the contaminated oil effluent; after that, EF, PF and Fenton processes have a good
 321 ability to reduce organic contaminants, respectively.

322 Considering the removal percentages obtained during these processes, it can be said that the slag fine particle
 323 catalyst of Khuzestan Steel Industries can be a suitable alternative to iron ions in Fenton-based processes as a
 324 catalyst. Also, cupal slag of steel industries of Khuzestan province, with suitable electrical resistance and current
 325 establishment, can be used as a cathode and anode in Fenton-based electrochemical process. Slag catalyst as a waste
 326 of Khuzestan steel industry has a very good potential for the treatment of petroleum industry effluents with very
 327 high organic pollution and resistant to biodegradation.

328 The results show that although Fenton-based processes can be used to reduce chemical oxygen demand pollution
 329 from petroleum industry desalination effluents; but the combined PEF process has a higher potential than other
 330 processes in removing chemical oxygen demand contamination from the effluent. The implementation of this system
 331 for the treatment of industrial effluents such as oil is recommended due to its high efficiency in reducing pollution,
 332 cost-effectiveness in industry, simplicity of work and ultimately less toxicity.

333

334 **Declarations**

335 -Ethics approval and consent to participate: 'Not applicable'

336 -Consent for publication: 'Not applicable'

337 -Availability of data and materials: The datasets used and analysed during the current study are available from the
 338 corresponding author on reasonable request.

339 -Competing interests: The authors declare that they have no competing interests.
340 -Funding: This research has been financially supported by the Research Council of Shahid Chamran University of
341 Ahvaz.
342 -Authors' contributions: All authors (F.E; P.T; SM.K and N.JH) conceived and designed the study. F.E carried out
343 the experiments. Both F.E and P.T analyzed the data, wrote the manuscript, and discussed the results. F.E, P.T,
344 SM.K and N.JH contributed to manuscript revision and approve it.
345 -Acknowledgements: We are grateful to the Research Council of Shahid Chamran University of Ahvaz for financial
346 support (GN: SCU.WI98.25891)

347 Reference

- 348 Aveiro, L. R. *et al.* (2018) 'Application and stability of cathodes with manganese dioxide nanoflowers supported on
349 Vulcan by Fenton systems for the degradation of RB5 azo dye', *Chemosphere*, 208, pp. 131–138. doi:
350 <https://doi.org/10.1016/j.chemosphere.2018.05.107>.
- 351 Babuponnusami, A. and Muthukumar, K. (2012a) 'Advanced oxidation of phenol: a comparison between Fenton,
352 electro-Fenton, sono-electro-Fenton and photo-electro-Fenton processes', *Chemical Engineering Journal*, 183,
353 pp. 1–9. doi: <https://doi.org/10.1016/j.cej.2011.12.010>.
- 354 Babuponnusami, A. and Muthukumar, K. (2012b) 'Removal of phenol by heterogenous photo electro Fenton-like
355 process using nano-zero valent iron', *Separation and Purification Technology*, 98, pp. 130–135. doi:
356 <https://doi.org/10.1016/j.seppur.2012.04.034>.
- 357 BAYAT, B. K. R., EBRAHIMI, M. and KEYVANI, B. (2013) 'Removal of Acid red 206 Dye in Pollutant Water by
358 ZnFe₂O₄/Bentonite as a Nanophotocatalyst in Batch Reactor Using Taguachi Method'.
- 359 Bokare, A. D. and Choi, W. (2014) 'Review of iron-free Fenton-like systems for activating H₂O₂ in advanced
360 oxidation processes', *Journal of Hazardous materials*, 275, pp. 121–135. doi:
361 <https://doi.org/10.1016/j.jhazmat.2014.04.054>.
- 362 Brillas, E. (2020) 'A review on the photoelectro-Fenton process as efficient electrochemical advanced oxidation for
363 wastewater remediation. Treatment with UV light, sunlight, and coupling with conventional and other photo-
364 assisted advanced technologies', *Chemosphere*, 250, p. 126198. doi:
365 <https://doi.org/10.1016/j.chemosphere.2020.126198>.
- 366 Brillas, E. and Martínez-Huitle, C. A. (2015) 'Decontamination of wastewaters containing synthetic organic dyes by
367 electrochemical methods. An updated review', *Applied Catalysis B: Environmental*, 166–167, pp. 603–643.
368 doi: <https://doi.org/10.1016/j.apcatb.2014.11.016>.
- 369 Byrappa, K. *et al.* (2008) 'Hydrothermal preparation of ZnO: CNT and TiO₂: CNT composites and their
370 photocatalytic applications', *Journal of Materials Science*, 43(7), pp. 2348–2355.
- 371 Chen, L. *et al.* (2011) 'Strong enhancement on Fenton oxidation by addition of hydroxylamine to accelerate the
372 ferric and ferrous iron cycles', *Environmental Science & Technology*, 45(9), pp. 3925–3930. doi:
373 <https://doi.org/10.1021/es2002748>.
- 374 Cho, M. *et al.* (2005) 'Different inactivation behaviors of MS-2 phage and Escherichia coli in TiO₂ photocatalytic
375 disinfection', *Applied and environmental microbiology*, 71(1), pp. 270–275. doi:
376 <https://doi.org/10.1128/AEM.71.1.270-275.2005>.
- 377 Coelho, A. *et al.* (2006) 'Treatment of petroleum refinery sourwater by advanced oxidation processes', *Journal of*
378 *Hazardous materials*, 137(1), pp. 178–184. doi: <https://doi.org/10.1016/j.jhazmat.2006.01.051>.

- 379 Coronado, J. M. *et al.* (2013) *Design of advanced photocatalytic materials for energy and environmental*
380 *applications*. Springer.
- 381 Dehghani, M. *et al.* (2014) 'Optimizing photo-Fenton like process for the removal of diesel fuel from the aqueous
382 phase', *Journal of Environmental Health Science and Engineering*, 12(1), pp. 1–7.
- 383 Deng, Y. and Zhao, R. (2015) 'Advanced oxidation processes (AOPs) in wastewater treatment', *Current Pollution*
384 *Reports*, 1(3), pp. 167–176.
- 385 Flores, N. *et al.* (2016) 'Degradation of trans-ferulic acid in acidic aqueous medium by anodic oxidation, electro-
386 Fenton and photoelectro-Fenton', *Journal of Hazardous Materials*, 319, pp. 3–12. doi:
387 <https://doi.org/10.1016/j.jhazmat.2015.11.040>.
- 388 Flores, N. *et al.* (2018) 'Treatment of olive oil mill wastewater by single electrocoagulation with different electrodes
389 and sequential electrocoagulation/electrochemical Fenton-based processes', *Journal of Hazardous Materials*,
390 347, pp. 58–66. doi: <https://doi.org/10.1016/j.jhazmat.2017.12.059>.
- 391 Ganiyu, S. O., Zhou, M. and Martínez-Huitle, C. A. (2018) 'Heterogeneous electro-Fenton and photoelectro-Fenton
392 processes: A critical review of fundamental principles and application for water/wastewater treatment', *Applied*
393 *Catalysis B: Environmental*, 235, pp. 103–129. doi: <https://doi.org/10.1016/j.apcatb.2018.04.044>.
- 394 Gaya, U. I. and Abdullah, A. H. (2008) 'Heterogeneous photocatalytic degradation of organic contaminants over
395 titanium dioxide: a review of fundamentals, progress and problems', *Journal of photochemistry and*
396 *photobiology C: Photochemistry reviews*, 9(1), pp. 1–12. doi:
397 <https://doi.org/10.1016/j.jphotochemrev.2007.12.003>.
- 398 Glaze, W. H. (1987) 'Drinking-water treatment with ozone', *Environmental Science & Technology*, 21(3), pp. 224–
399 230. doi: <https://doi.org/10.1021/es00157a001>.
- 400 Glaze, W. H., Kang, J.-W. and Chapin, D. H. (1987) 'The chemistry of water treatment processes involving ozone,
401 hydrogen peroxide and ultraviolet radiation'. doi: <https://doi.org/10.1080/01919518708552148>.
- 402 Gönder, Z. B. *et al.* (2010) 'Optimization of filtration conditions for CIP wastewater treatment by nanofiltration
403 process using Taguchi approach', *Separation and Purification Technology*, 70(3), pp. 265–273. doi:
404 <https://doi.org/10.1016/j.seppur.2009.10.001>.
- 405 Guelfi, D. R. V *et al.* (2019) 'Ensuring the overall combustion of herbicide metribuzin by electrochemical advanced
406 oxidation processes. Study of operation variables, kinetics and degradation routes', *Separation and Purification*
407 *Technology*, 211, pp. 637–645. doi: <https://doi.org/10.1016/j.seppur.2018.10.029>.
- 408 Ifelebuegu, A. O. and Ezenwa, C. P. (2011) 'Removal of endocrine disrupting chemicals in wastewater treatment by
409 Fenton-like oxidation', *Water, Air, & Soil Pollution*, 217(1–4), pp. 213–220.
- 410 Ikai, H. *et al.* (2010) 'Photolysis of hydrogen peroxide, an effective disinfection system via hydroxyl radical
411 formation', *Antimicrobial agents and chemotherapy*, 54(12), pp. 5086–5091. doi:
412 <https://doi.org/10.1128/AAC.00751-10>.
- 413 Jaafarzadeh, N., Ghanbari, F. and Moradi, M. (2015) 'Photo-electro-oxidation assisted peroxydisulfate for
414 decolorization of acid brown 14 from aqueous solution', *Korean Journal of Chemical Engineering*, 32(3), pp.
415 458–464.
- 416 Khataee, A. R. and Zarei, M. (2011) 'Photocatalysis of a dye solution using immobilized ZnO nanoparticles
417 combined with photoelectrochemical process', *Desalination*, 273(2–3), pp. 453–460.
- 418 Khataee, A. R., Zarei, M. and Asl, S. K. (2010) 'Photocatalytic treatment of a dye solution using immobilized TiO₂
419 nanoparticles combined with photoelectro-Fenton process: Optimization of operational parameters', *Journal of*
420 *Electroanalytical Chemistry*, 648(2), pp. 143–150. doi: <https://doi.org/10.1016/j.jelechem.2010.07.017>.
- 421 Komtchou, S. *et al.* (2017) 'Removal of atrazine and its by-products from water using electrochemical advanced
422 oxidation processes', *Water Research*, 125, pp. 91–103. doi: <https://doi.org/10.1016/j.watres.2017.08.036>.

- 423 Lopez-Saavedra, N. *et al.* (2018) 'Experimental data on the degradation of caffeine by photo-electro-fenton using
424 BDD electrodes at pilot plant', *Data in brief*, 21, pp. 1709–1715. doi: <https://doi.org/10.1016/j.dib.2018.10.174>.
- 425 Meriç, S., Kaptan, D. and Ölmez, T. (2004) 'Color and COD removal from wastewater containing Reactive Black 5
426 using Fenton's oxidation process', *Chemosphere*, 54(3), pp. 435–441. doi:
427 <https://doi.org/10.1016/j.chemosphere.2003.08.010>.
- 428 Milkey, K. R. *et al.* (2014) 'Comparison between Taguchi Method and Response Surface Methodology (RSM) in
429 Modelling CO₂ Laser Machining', *Jordan Journal of Mechanical & Industrial Engineering*, 8(1).
- 430 Moreira, F. C. *et al.* (2017) 'Electrochemical advanced oxidation processes: A review on their application to
431 synthetic and real wastewaters', *Applied Catalysis B: Environmental*, 202, pp. 217–261. doi:
432 <https://doi.org/10.1016/j.apcatb.2016.08.037>.
- 433 Mousavi, S. A. *et al.* (2010) 'Fenton oxidation efficiency in removal of detergents from water', *J. of Water and
434 Wastewater*, 72, pp. 16–23.
- 435 Mousset, E. *et al.* (2017) 'A new 3D-printed photoelectrocatalytic reactor combining the benefits of a transparent
436 electrode and the Fenton reaction for advanced wastewater treatment', *Journal of Materials Chemistry A*, 5(47),
437 pp. 24951–24964. doi: 10.1039/C7TA08182K.
- 438 Nidheesh, P. V. and Gandhimathi, R. (2014) 'Comparative Removal of Rhodamine B from Aqueous Solution by
439 Electro-Fenton and Electro-Fenton-Like Processes', *CLEAN–Soil, Air, Water*, 42(6), pp. 779–784. doi:
440 <https://doi.org/10.1002/clen.201300093>.
- 441 Nidheesh, P. V., Zhou, M. and Oturan, M. A. (2018) 'An overview on the removal of synthetic dyes from water by
442 electrochemical advanced oxidation processes', *Chemosphere*, 197, pp. 210–227. doi:
443 <https://doi.org/10.1016/j.chemosphere.2017.12.195>.
- 444 Oh, S.-Y. *et al.* (2005) 'Zero-valent iron pretreatment for enhancing the biodegradability of RDX', *Water research*,
445 39(20), pp. 5027–5032.
- 446 Oriol, R. *et al.* (2019) 'A hybrid photoelectrocatalytic/photoelectro-Fenton treatment of Indigo Carmine in acidic
447 aqueous solution using TiO₂ nanotube arrays as photoanode', *Journal of Electroanalytical Chemistry*, 847, p.
448 113088.
- 449 Ou, B. *et al.* (2019) 'Treatment of polyaniline wastewater by coupling of photoelectro-Fenton and heterogeneous
450 photocatalysis with black TiO₂ nanotubes', *ACS Omega*, 4(6), pp. 9664–9672.
- 451 Padmanabhan, P. V. A. *et al.* (2006) 'Nano-crystalline titanium dioxide formed by reactive plasma synthesis',
452 *Vacuum*, 80(11–12), pp. 1252–1255. doi: <https://doi.org/10.1016/j.vacuum.2006.01.054>.
- 453 Sharma, A., Ahmad, J. and Flora, S. J. S. (2018) 'Application of advanced oxidation processes and toxicity
454 assessment of transformation products', *Environmental research*, 167, pp. 223–233. doi:
455 <https://doi.org/10.1016/j.envres.2018.07.010>.
- 456 Stepnowski, P. *et al.* (2002) 'Enhanced photo-degradation of contaminants in petroleum refinery wastewater', *Water
457 research*, 36(9), pp. 2167–2172. doi: [https://doi.org/10.1016/S0043-1354\(01\)00450-X](https://doi.org/10.1016/S0043-1354(01)00450-X).
- 458 Steter, J. R., Brillas, E. and Sirés, I. (2016) 'On the selection of the anode material for the electrochemical removal
459 of methylparaben from different aqueous media', *Electrochimica Acta*, 222, pp. 1464–1474. doi:
460 <https://doi.org/10.1016/j.electacta.2016.11.125>.
- 461 Suraj, P. *et al.* (2019) 'Taguchi optimization of COD removal by heterogeneous Fenton process using copper ferro
462 spinel catalyst in a fixed bed reactor—RTD, kinetic and thermodynamic study', *Journal of Environmental
463 Chemical Engineering*, 7(1), p. 102859. doi: <https://doi.org/10.1016/j.jece.2018.102859>.
- 464 Takeuchi, M., Hidaka, M. and Anpo, M. (2012) 'Efficient removal of toluene and benzene in gas phase by the
465 TiO₂/Y-zeolite hybrid photocatalyst', *Journal of Hazardous Materials*, 237–238, pp. 133–139. doi:
466 10.1016/j.jhazmat.2012.08.011.

467 Tambosi, J. L. *et al.* (2006) ‘Treatment of paper and pulp wastewater and removal of odorous compounds by a
468 Fenton-like process at the pilot scale’, *Journal of Chemical Technology & Biotechnology: International*
469 *Research in Process, Environmental & Clean Technology*, 81(8), pp. 1426–1432. doi:
470 <https://doi.org/10.1002/jctb.1583>.

471 Thiam, A. and Salazar, R. (2019) ‘Fenton-based electrochemical degradation of metolachlor in aqueous solution by
472 means of BDD and Pt electrodes: influencing factors and reaction pathways’, *Environmental Science and*
473 *Pollution Research*, 26(3), pp. 2580–2591. doi: 10.1007/s11356-018-3768-2.

474 Tony, M. A. *et al.* (2009) ‘Photo-catalytic degradation of an oil-water emulsion using the photo-fenton treatment
475 process: Effects and statistical optimization’, *Journal of Environmental Science and Health Part A*, 44(2), pp.
476 179–187.

477 Villanueva-Rodríguez, M. *et al.* (2014) ‘Discoloration and organic matter removal from coffee wastewater by
478 electrochemical advanced oxidation processes’, *Water, Air, & Soil Pollution*, 225(12), pp. 1–11.

479 Wang, N. *et al.* (2016) ‘A review on Fenton-like processes for organic wastewater treatment’, *Journal of*
480 *Environmental Chemical Engineering*, 4(1), pp. 762–787. doi: <https://doi.org/10.1016/j.jece.2015.12.016>.

481 Xing, Z., Sun, D. and Yu, X. (2010) ‘Treatment of antibiotic fermentation wastewater using the combined polyferric
482 sulfate coagulation with Fenton-like oxidation’, *Environmental progress & sustainable energy*, 29(1), pp. 42–
483 51.

484 Ye, Z. *et al.* (2019) ‘Photoelectro-Fenton as post-treatment for electrocoagulated benzophenone-3-loaded synthetic
485 and urban wastewater’, *Journal of Cleaner Production*, 208, pp. 1393–1402. doi:
486 <https://doi.org/10.1016/j.jclepro.2018.10.181>.

487 Yonar, T. and Kurt, A. (2017) ‘Treatability studies of hospital wastewaters with AOPs by Taguchi’s experimental
488 design’, *Glob Nest J*, 19, pp. 505–510.

489 Zhang, L. *et al.* (2009) ‘Photocorrosion suppression of ZnO nanoparticles via hybridization with graphite-like
490 carbon and enhanced photocatalytic activity’, *The Journal of Physical Chemistry C*, 113(6), pp. 2368–2374.

491